We are IntechOpen, the world's leading publisher of Open Access books Built by scientists, for scientists

4,800
Open access books available

122,000
International authors and editors

135M
Downloads

Our authors are among the

154
Countries delivered to

TOP 1%
most cited scientists

12.2%
Contributors from top 500 universities

CLARIVATE ANALYTICS BOOK CITATION INDEX INDEXED

WEB OF SCIENCE™

Selection of our books indexed in the Book Citation Index in Web of Science™ Core Collection (BKCI)

Interested in publishing with us?
Contact book.department@intechopen.com

Numbers displayed above are based on latest data collected.
For more information visit www.intechopen.com

14

Rainfall Prediction Using Teleconnection Patterns Through the Application of Artificial Neural Networks

Gholam Abbas Fallah-Ghalhari
Sabzevar Tarbiat Moallem University
I.R of Iran

1. Introduction

All aspects of human life are, directly or indirectly, affected by climatic processes. This effect is especially noticeable in such fields as agriculture, irrigation, economy, telecommunications, transportation, traffic, air pollution and military industries (Haltiner & Williams 1980).

A number of researchers have studied the possibility of forecasting rainfall several months in advance using climate indices such as SOI, PDOI and NPI (e.g. Silverman and Dracup 2000).

A well-known atmospheric phenomenon is the Southern Oscillation (SO). The SO is an atmospheric see-saw process in the tropical Pacific sea level pressure between the eastern and western hemispheres associated with the El Niño and La Niña oceanographic features. The oscillation can be characterized by a simple index, the Southern Oscillation Index (SOI). (Kawamura et al., 1998). The Pacific Decadal Oscillation index (PDOI) is the leading principal component of monthly sea surface temperature (SST) anomalies in the North Pacific Ocean north of 20°N (Zhang et al., 1997; Mantua et al., 1997). Trenberth and Hurrell (1994) have defined the North Pacific Index (NPI) as the area-weighted sea level pressure over the region 30°N to 65°N, 160°E to 140°W to measure the decadal variations of atmosphere and ocean in the north Pacific.

Furthermore, the existence of substantial databases of sea surface temperature anomalies (SST) opens the possibility of using these data to forecast rainfall several months in advance. Most of the research carried out in this area has used traditional statistical methods such as linear correlation or time series methods to identify the significant variables. These methods test for a linear relationship between the independent variables and rainfall, whereas the relationships are more likely to be non-linear as the underlying processes are themselves non-linear (Iseri et al. 2005).

Long-term rainfall prediction is very important to countries thriving on agro-based economy. In general, climate and rainfall are highly non-linear phenomena in nature giving rise to what is known as butterfly effect (Abraham et al. 2001). In their quest for new ways of predicting important meteorological factors, researchers have devised and developed techniques such as intelligent methods, which are viable and flexible means independent of system dynamic models.

Pongracz & Bartholy (2006) designed a model of monthly rainfall in Hungary using types of atmospheric circulation patterns and ENSO (El Niño - Southern Oscillation) index. To this end, they used a modeling technique based on fuzzy rules to establish a relationship between inputs and rainfall. Their results indicated that the model based on fuzzy rules provides an excellent means for the prediction of statistical features of rainfall using monthly occurrence of types of daily circulation pattern and delayed SOI.

Halid & Ridd (2002) used the fuzzy logic to design a model and predict local rainfall in January at Hasanuddin airport, Indonesia, which is the largest rice-producing area in the country. Their results indicated that, compared to other statistical models, the fuzzy logic model is more useful for the prediction of rainfall in January. Choi (1999) used neural networks and the Geographical Information System to forecast rainfall. The results indicated the efficiency of the Geographical Information System and neural networks in rainfall forecast. Cavazos (2000) used neural networks to forecast daily rainfall. The parameters which were used included the thickness between 500 and 1000 hecto-Pascal levels, the altitude of 500 hPa levels, and the humidity of 700 hPa levels. The outcomes indicated the efficiency of neural networks in the prediction of rainfall. Maria et al (2005) used neural networks and regression models to forecast rainfall in Sao Paulo, Brazil. The parameters they used included: potential temperature, vertical wind component, specific humidity, precipitable water, relative vorticity and humidity flux divergence. The results indicated the efficiency of both methods in forecasting rainfall.

One of the most crucial issues of global climatic variability is its effect on water resources. If more accurate predictions of rainfall were possible, this would enable more efficient utilization of water resources. However, long-term rainfall prediction models are still unsatisfactory, whereas short-term rainfall prediction models have undergone significant development. The probable reasons for the difficulties in conducting long-term rainfall prediction are the complexity of atmosphere-ocean interactions and the uncertainty of the relationship between rainfall and hydro meteorological variables. So far, long-term climate prediction using numerical models has not demonstrated useful performance, and statistical models have shown better performance than numerical models (Zwiers & Von Storch 2004). Consequently, in this study Artificial Neural Networks and linear regression models have been applied to nonlinear and linear statistical prediction.

Due to the significance of rainfall in many decision making processes such as water resources management and agriculture, the present study aims to find out the relationship between large-scale climatic synoptic patterns and regional rainfall using such synoptic patterns as sea level temperature and temperature difference, sea level pressure and pressure difference, precipitable water, air temperature at 700-hPa level, the thickness between 500 and 1000-hPa levels and the relative humidity at 300-hPa level.

2. Data and methods

2.1 Data

2.1.1 Study area

The region studied in this research is Khorasan Razavi Province. The time series studied is the average rainfall from April to June during 38 years. The data of spring rainfall for each

year includes the rainfall in 34 visibility, climatology and rainfall measurement stations provided by the Weather Bureau and the Power Ministry. Of these, 24 stations are rainfall measurement stations of the Power Ministry and the rest belong to the Weather Bureau. Fig. 1 represents the map of the studied area and the name of the relevant stations. To compensate for some defects in rainfall data, subtractions and ratios method have used. Run test was also used to test the homogeneity of the data. The analysis of *runs* within a sequence is applied in statistics in many ways (for examples see Feller 1968 & Ducan 1974). The term *run* may in general be explained as a succession of items of the same class. Many concepts to analyze runs in a series of data have been studied. The main concepts are based on (i) the analysis of the total number of runs of a given class (see Guibas and Odlyzko 1980 and Knuth 1981) and (ii) examinations about the appearance of long runs (see Feller 1968, Guibas and Odlyzko 1980 and Wolfowitz 1944).

Fig. 1. Map of the region under study and selected stations (Fallah Ghalhary et al, 2010)

2.1.2 Climatological data

The data used in this study are:

1. 34 Rainfall station data for the seasonal rainfall (April – June) were obtained from Iranian Meteorological organization. All of these stations are in the north eastern region of Iran.
2. Large-scale ocean and atmospheric circulation variables such as Sea Surface Temperature (SST), Sea Level Pressure(SLP), the difference Sea Level Pressure, the difference Sea Surface Temperature between surface and 1000 hPa level, relative humid at 300 hPa level, geopotential height at 500 hPa level, air temperature at 850 hPa level during months (Oct-Mar). These data were obtained from NCEP/NCAR Re-analysis data. These data sets span the period of 1948 – current, covering the globe on a 2.5 × 2.5 grid and available at http://www.cdc.noaa.gov National Oceanic and Atmospheric Administration (NOAA) website. Table 1 summarizes the data used in this study.

Data	source	time	year
Rainfall station data	Iranian Meteorological organization	April – June	1970-2007
NCEP/NCAR Re-analysis data	Large-scale ocean and atmospheric circulation variables	Oct-Mar	1970-2007

Table 1. Summaries of the data used in this study

2.2 Methods

2.2.1 Spatial prediction and kriging

The need to obtain accurate predictions from observed data can be found in all scientific disciplines. Those that have embraced statistical notions of random variation are able to do this by exploiting the statistical dependence among the data and the variables(s) to be predicted. However, the statistical approach has not been without its detractors; for example, Philip and Waston (1986) argue that geostatistics is unhelpful for solving problems in mining and geology. Their article and the accompanying discussions are worth perusing.

It is helpful to explain first the terms used in the title of this chapter. Let $\{Z(s): s \in D \subset R^d\}$ be a random function (or process), from which n data $Z(s_1), \ldots, Z(s_n)$ are collected. The data are used to perform inference on the process, here, to predict some known functional $g(\{Z(s): s \in D\})$ [or, more simply, $g(Z(.))$] of the random function Z (.). For example, point prediction assumes $g(Z(.))=Z(S_0)$, where S_0 is a known spatial location. g is mostly real-valued. Sometimes interest is not in Z (.), but in a "noiseless" version of it.

Suppose that

$$Z(s) = S(s) + \in (s), s \in D, \quad (1)$$

Where $\in$ (.) is a white-noise measurement-error process. In this case, one is interested in predicting a known functional g(S (.)) of the noiseless random function S (.).

Spatial prediction refers to prediction either g(Z(.)) or g(S(.)) from data $Z(s_1), \ldots, Z(s_n)$ observed at known spatial locations $s_1, \ldots, s_n$.

Notice that my terminology encompasses the temporal notions of smoothing (or interpolation), filtering, and prediction (e.g., Lewis, 1986, PP. 36), which rely on time-

ordering for their distinction. If temporal data are available from the past up to and including the present, smoothing refers to prediction of g(S (.)) at time points in the past, filtering refers to prediction of g(S (.)) at the present time and prediction refer to prediction of g(S (.)) at time points in the future. In this paper, the word "estimation" will be used exclusively for inference on fixed but unknown parameters; "prediction" is reserved for inference on random quantities.

Kriging is a minimum-mean-squared-error method of spatial prediction that (usually) depends on the second-order properties of the process Z (.).

Matheron (1963) named this method of optimal spatial linear prediction after D. G. Krige, a South African mining engineer who, in the 1950s, developed empirical methods for determining true ore-grade distributions from distributions based on sampled ore grades (e. g., Krige, 1951). However, the formulation of optimal spatial linear prediction did not come from krige's work. (See Matheron, 1971, pp. 117-119, and Cressie, 1990, for the extent of the early work of Krige.) The contributions of Wold (1938), Kolmogorov (1941), and Wiener (1949) all contain optimal linear prediction equations that reflect the notion that observations closer to the prediction point (for them, closer in time) should be given more weight in the predictor.

At the same time as geostatististics was developing in mining engineering under G. Matheron in France, the very same ideas developed in meteorology under L. S. Gandin (Gandin, 1963) in the Soviet Union. The original (and simultaneous) contribution of these authors was to put optimal linear prediction (in terms of variogram) into a spatial setting. Gandins' name for his approach was *objective analysis*, and he used the terminology *optimum interpolation* instead of Kriging. Details of the origins of Kriging are set out in Cressie (1990) and Cressie (1993).

2.2.1.1 Observational and spatial scale

The following model is useful. Suppose that the data ($Z(S_1)\ldots Z(S_n)$) represent Z values at points of $D \subset R^d$, and that they are modeled as a partial realization of the random process:

$$\{Z(s): S \in D \subset R^d\}, \tag{2}$$

Which satisfies the decomposition

$$Z(s) = \mu(s) + W(s) + \eta(s) + \in (s), \; s \in D\,, \tag{3}$$

Where:

$\mu(.) \equiv E(Z(.))$ Is the deterministic mean structure that will be called *large-scale variation.*

W (.) is a zero-mean, L_2-continues [*i.e.*, $E(W(s+h)-W(s))^2 \to 0 \; as \; \|h\| \to 0$], intrinsically stationary process whose variogram rang (if it exist) is larger than min $\{\|s_i - s_j\| : 1 \le i < j \le n\}$. Call W (.) *smooth small-scale variation*.

η (.) Is a zero-mean, intrinsically stationary process, independent of W, whose variogram rang exists and is smaller than min $\{\|s_i - s_j\| : 1 \le i < j \le n\}$. Call $\eta(.)$ *microscale variation*.

∈ (.) is a zero-mean white-noise process, independent of W and η call ∈ (.) measurement error or noise, and denote var (∈ (s))= C_{ME}. There are occasions when ∈ (.) may possess more structure than that of white noise (e.g., Laslett and McBratney, 1990).

In notation as follow,

$$2\,y_Z(.) = 2\,y_W(.) + 2\,y_\eta(.) + 2c_{ME}. \tag{4}$$

The quantities C_{ME} and $\gamma_Z(h)$, $\|h\|$ larger, are pertinent to the observational scale; the other quantities contain information on the spatial scale.

From the decomposition (3), write

$$Z(s) = S(s) + \in (s),\ s \in D, \tag{5}$$

Where the "signal" or smooth process S (.) is given by $S(.) \equiv \mu(.) + W(.) + \eta(.)$. The S process is often referred to as the noiseless version of the Z process or, in the engineering literature, as the *state* process. Also, write

$$Z(s) \equiv \mu(s) + \delta(s),\ s \in D, \tag{6}$$

Where the correlated error process $\delta(.)$ is given by $\delta(.) \equiv W(.) + \eta(.) + \in(.)$. When the Correlation of $\delta(s)$ white $\delta(s+h)$ can be written as a function of $h/\alpha(h)$, where $0 < \alpha(h) < \infty$, then $\alpha(h)$ is sometimes called the *spatial correlation scale* of the process in direction h (Cressie, 1993).

2.2.1.2 Ordinary kriging

Ordinary Kriging produced better estimates than simple Kriging because of the non-stationarity of the data. The original data set had large areas where the values were low and large areas where the values were high. Simple Kriging requires the mean value of the data set to be provided, whereas ordinary Kriging calculates a mean for each individual block, based on the samples included in estimate. The local mean appears to be more meaningful in a situation where the global mean is not constant (Weber and Englund, 1992).

The word "Kriging" is synonymous with "optimal prediction" (as a noun) or with "optimally predicting" (as the present participle of a verb). In other words, it refers to making inferences on unobserved values of the random process Z (.) given by (2) or of S (.) given by (5) from data:

$$Z \equiv (Z(S_1),...,Z(S_n)) \tag{7}$$

Observed at known spatial locations $\{s_1,\ldots,s_n\}$.

Denote the generic predictor of g (Z (.) or g(S (.)) by:

$$P(Z; g) \tag{8}$$

Choice of a good predictor will depend on the geometry and location of the region of space where prediction is desired and weather it is the Z process or the S process that is to be predicted. When g (Z (.)) = Z (B) $[\equiv \int_B Z(u)du/|B|]$ or g(S (.)) = S (B), write (3.2.3) as p (Z; B). In the special case of B = $\{s_0\}$, write (8) as p (Z; s_0).

Ordinary Kriging (Matheron, 1971; Journel and Huijbregts, 1978) refers to spatial prediction under the following two assumptions.

Model Assumption. In (6)

$$Z(s) = \mu + \delta(s), \quad s \in D, \mu \in \mathrm{R}, \text{ and } \mu \text{ unknown.} \tag{9}$$

Predictor Assumption.

$$p(Z;B) = \sum_{i=1}^{n} \lambda_i Z(s_i), \quad \sum_{i=1}^{n} \lambda_i = 1. \tag{10}$$

This latter condition, which the coefficients of the linear predictor sum to 1, guarantees uniform unbiasedness. E (p (Z; B)) = $\mu = E(Z(B))$, for all $\mu \in$ R.

There is a version of Kriging called simple Kriging, where μ in (9) is known and the coefficients are not constrained to sum to 1.

Hence, if

$$g(Z(.)) = Z(B) \equiv \begin{cases} \int_B Z(u)du / |B|, & |B| > 0 \\ ave\{Z(u) : u \in B\}, & |B| = 0 \end{cases} \tag{11}$$

Then the optimal p (. ; B) will minimize the mean-squared prediction error

$$\sigma_e^2 \equiv E(Z(B) - p(Z;B))^2 \tag{12}$$

Over the class of linear predictors $\sum_{i=1}^{n} \lambda_i Z(s_i)$ that satisfy $\sum_{i=1}^{n} \lambda_i = 1$ (Cressie, 1993).

2.2.1.3 Kriging and calculating the average regional rainfall

In this research, we have used from ordinary Kriging for obtaining the average regional rainfall in the area under study. Kriging is the estimation procedure used in geostatistics using known values and a semivariogram to determine unknown values. It was named after D. G. Krige from South Africa. The procedures involved in Kriging incorporate measures of error and uncertainty when determining estimations. Based on the semivariogram used, optimal weights are assigned to unknown values in order to calculate unknown ones. Since the variogram changes with distance, the weights depend on the known sample distribution (Davis 1990).

The final goal of studying spatial changes of rainfall is to simulate the changes in rainfall data in the spatial dimension in order to pave the way for attaining other goals such as forecasting rainfall and getting necessary information for the long-term analysis of rainfall in every region in the area under study. As mentioned before, Kriging method used in this study to calculate the average regional rainfall. The following steps were taken to obtain the time series of average regional rainfall:

1. Making input files for the Arc GIS 9.2 software
2. Obtaining the experimental variogram
3. Analyzing and drawing annual spatial changes of rainfall in the region
4. Obtaining the values of annual average rainfall in the region under study
5. Making time series of rainfall in the region under study.

Fig.2 for example shows the diagram of the Variogram using spherical model to estimate of the average regional rainfall for the year of 2007.

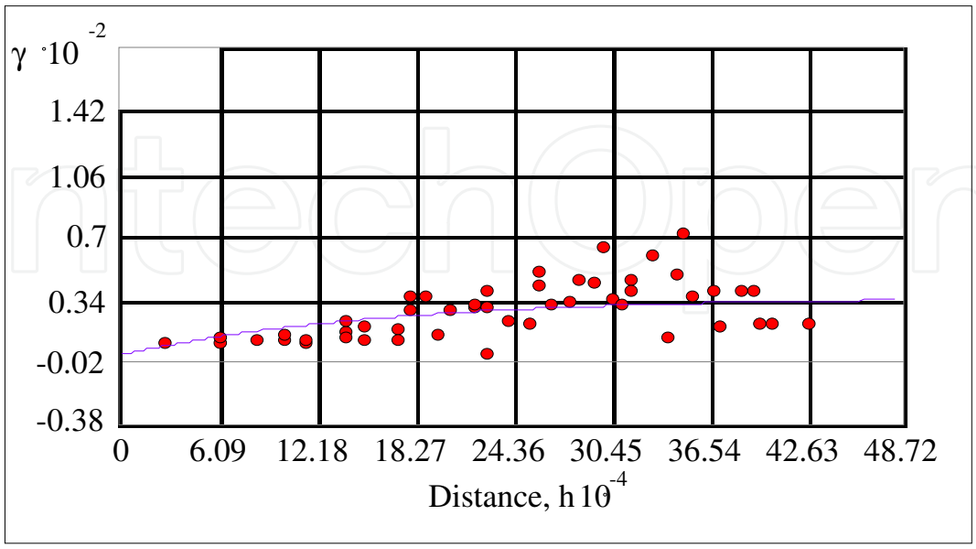

Fig. 2. Variogram diagram using spherical model to estimate of the average regional rainfall for year of 2007. Units on the horizontal and vertical axes are meter and square millimeter respectively.

2.2.2 Determining seasonal rainfall and predictors

The predictors studied in this research are classified into two groups: meteorological parameters at ground level and meteorological parameters at upper levels of the atmosphere. Table 2 shows these parameters.

Upper level of atmosphere	Ground level
Air temperature at 700-hPa level	Sea level pressure
the thickness between 500 and 1000hPa levels	Sea level pressure difference
Relative humidity of 300-hPa level	Sea level temperature
	Temperature difference between sea level and 1000-hPa level
	Zonal wind
	Meridional wind
	Precipitable water

Table 2. Meteorological Parameters used in this study

One distinctive scenario is considered in this study. This scenario uses input data with 6 months lags to investigate the possibility of forecasting more than 3 months in advance.

One of the objectives of this study is the identification of a possible relationship between rainfall in Iran and climatic predictors, using Pearson's correlation coefficient. The other objective is to verify the forecasts produced using the predictors identified with Pearson's correlation coefficient.

Seasonal rainfall and predictors have been determined using the average of the values of a predictor in order to predict the amount of seasonal rainfall. We made sure that the seasons of the predictor do not include months with rainfalls.

Since we aimed to investigate the relation between meteorological parameters and spring rainfall in this study (spring rainfall is very important in dry land cultivation and water recourses management), we used the average value of meteorological predictors in the period between October and March as the time series of the predictors and the average rainfall in the period between April and June as the rainfall time series.

To analyze the parameters of the upper levels of the atmosphere as well as three ground parameters, i.e. zonal wind, meridional wind and precipitable water in the present study, we used 5°×5° and 10°×10° degrees spatial resolution. The study areas, where meteorological parameters at ground level and upper levels of atmosphere have been factor-analyzed, are located between 0-80 °E and 10-50 °N in 5°×5° degrees spatial resolution and between 0-100 °E and 0-70 °N in 10°×10° degrees spatial resolution. The area includes regions where changes in the pattern of temperature, pressure, humidity, and wind speed affect Iranian rainfall (Fig. 3).

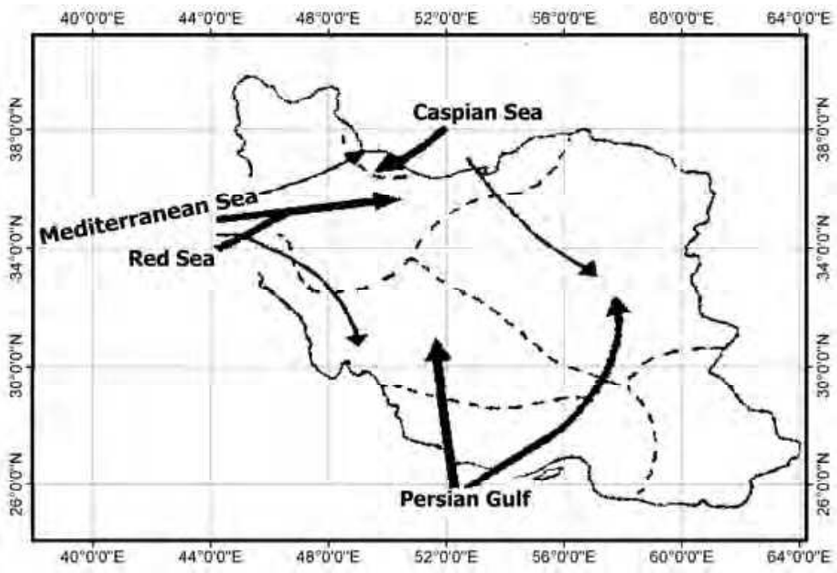

Fig. 3. Humidity sources of Iranian rainfalls in the spring season (Alijani, 2006). the wider arrows have more contribution.

For other parameters at ground level including pressure, temperature, pressure difference and temperature difference between sea level and 1000-hPa level, some points has been selected. That is, points were selected and analyzed in different parts of the seas, which were known to affect the climate of Iran from previous studies by other researchers (Nazemosadat & Cordery 2000, Alijani 2006).

We have used factor analysis to analyze the meteorological parameters at upper atmosphere and ground levels (zonal wind, meridional wind and precipitable water). The field of factor analysis involves the study of order and structure in multivariate data. The field includes both theory about the underlying constructs and dynamics which give rise to observed

phenomena, and methodology for attempting to reveal those constructs and dynamics from observed data. Factor analysis is preferable to principal components analysis. Components analysis is only a data reduction method. It became common decades ago when computers were slow and expensive to use; it was a quicker, cheaper alternative to factor analysis (Gorsuch 1997). It is computed without regard to any underlying structure caused by latent variables; components are calculated using all of the variance of the manifest variables, and all of that variance appears in the solution (Ford et al. 1986).

In this statistical method designed to reduce the number of variables, the initial parameters are transformed into independent variables based on their correlation coefficients. These independent variables are called factors. The value of each of the observations in the new factors is calculated as factorial score. Hence, rather than true values of observations, their scores in new components are used as new criteria for clustering. The advantage of this method is that while it reduces the number of variables, it preserves the initial variance of the main data (Alijani 2006).

As mentioned above, to find out the relation between rainfall in the region under study and the changes in meteorological parameters of pressure, temperature, pressure difference and temperature difference, the points in different parts of the seas have been studied, which are supposed to affect the climate of Iran. These include points in the Mediterranean, Persian Gulf, Oman Sea, Aden Gulf, Arab Sea, Red Sea, Black Sea, the Adriatic, Aral Lake, Indian Ocean, The Atlantic, North Sea and Siberia (Fig. 4). Table 3 shows Time series of average regional rainfall (from April to June) and value of predictors.

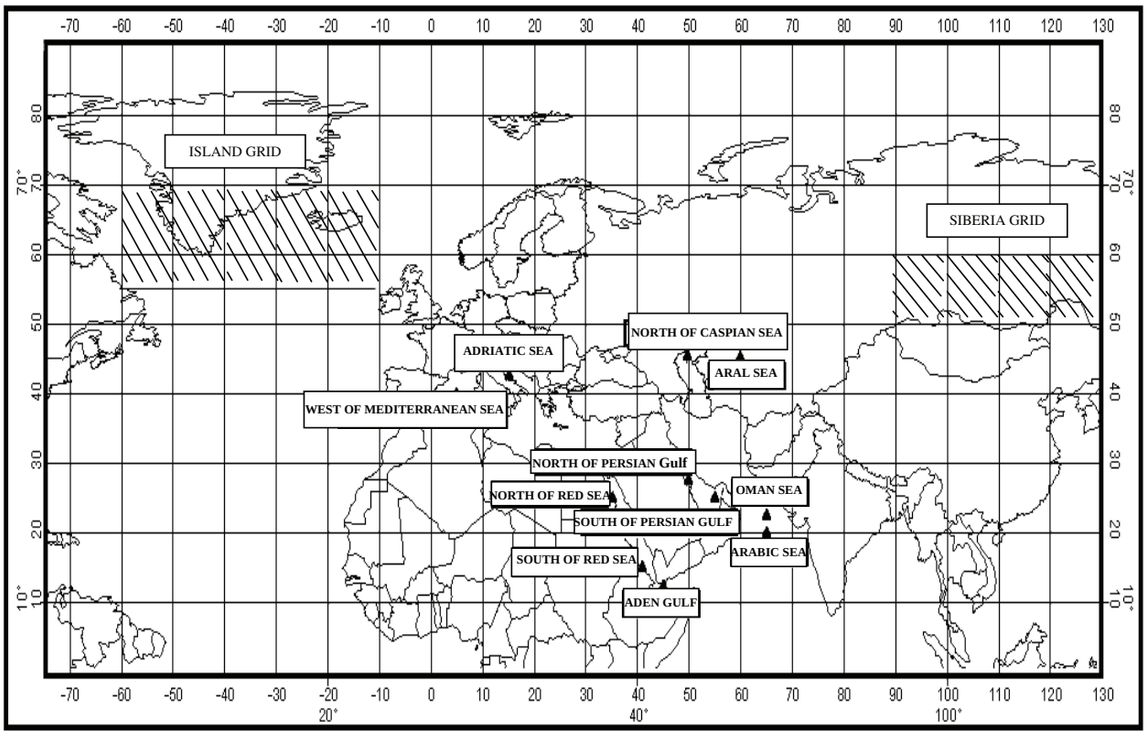

Fig. 4. Name and coordinates that have used for relation between rainfall and Remote Linkage Controlling (Fallah Ghalhary et al, 2010)

Year	Rainfall	x1	x2	x3	x4	x5	x6	x7	x8	x9	x10	x11	x12	x13	x14
1970	20.40	-1.15	0.27	0.17	-0.73	-1.65	-0.97	-1.63	-1.23	-1.28	0.20	-6.57	36.53	33.29	31.94
1971	17.35	-0.84	0.68	0.30	-0.19	-1.22	-1.30	-1.60	-1.46	0.02	0.07	-7.10	36.05	32.71	22.39
1972	27.93	-1.88	-0.46	0.18	1.81	-0.26	-0.03	-0.23	-0.30	-0.11	-1.80	-7.42	33.17	35.53	30.18
1973	30.96	-0.57	-0.45	-0.14	0.71	1.03	0.44	0.33	-0.22	0.29	-0.78	-7.35	36.44	36.31	27.58
1974	28.46	-0.65	-0.40	0.01	-0.58	-0.11	-1.03	-0.71	-1.04	0.46	-0.83	-7.12	34.52	32.60	25.40
1975	20.53	-0.67	-1.40	0.00	-0.08	0.51	-0.41	-0.06	-0.18	-0.69	-0.95	-7.04	34.65	34.97	24.05
1976	21.07	-1.80	-0.56	-0.26	0.84	-1.02	-1.54	-1.41	-0.83	0.16	-1.20	-7.83	34.08	35.95	28.07
1977	33.50	0.30	-1.02	0.12	-0.88	0.35	-1.02	-0.41	0.53	1.02	0.20	-5.94	36.75	34.26	34.78
1978	20.54	-0.56	0.38	0.23	0.49	0.91	0.49	-0.12	1.41	-1.49	0.11	-6.70	36.26	30.80	29.98
1979	20.88	-0.92	-0.18	0.32	-0.30	-0.12	0.16	-0.18	0.83	-0.51	0.61	-6.28	35.77	31.06	27.98
1980	17.18	0.28	-0.67	0.04	0.25	-0.14	0.10	0.18	-0.13	-1.44	0.18	-7.19	34.88	39.84	30.05
1981	22.40	0.28	-1.65	0.16	-0.02	-0.21	-0.20	-0.18	0.31	-1.41	1.10	-6.59	36.24	35.34	26.22
1982	28.08	-0.52	-0.06	0.02	-0.25	0.65	0.62	0.96	0.79	-0.91	-0.33	-7.10	35.36	34.97	26.45
1983	24.48	-0.27	-0.35	-0.38	-0.11	2.71	0.94	2.71	2.72	0.40	-1.33	-6.65	34.87	37.71	29.28
1984	19.19	-0.44	0.46	-0.02	0.15	0.21	0.02	0.54	0.53	-0.13	0.34	-6.98	39.57	31.10	22.57
1985	17.83	0.34	-1.00	0.04	-1.46	0.40	-1.21	-0.18	-0.09	1.01	0.07	-7.41	36.57	32.78	25.18
1986	16.11	-1.53	0.22	-0.09	0.10	0.26	-0.17	0.40	0.12	-0.05	0.14	-6.75	36.04	30.92	23.09
1987	20.41	-0.05	-0.21	-0.04	-0.46	0.95	1.44	1.60	1.60	-1.87	0.39	-7.66	36.27	28.92	20.10
1988	23.79	-0.37	1.09	-0.06	-0.27	-0.14	-1.12	-0.08	0.29	0.42	0.74	-6.64	39.42	32.70	24.55
1989	19.86	-0.46	0.00	-0.20	0.69	0.66	-0.07	0.35	0.73	1.77	-0.21	-6.91	35.09	25.91	20.53
1990	14.07	-0.13	1.26	-0.26	-0.54	0.75	0.66	0.51	0.48	1.00	0.01	-5.90	35.91	36.22	26.97
1991	17.73	0.53	-0.54	-0.07	-0.38	-0.59	0.59	-0.55	0.16	-0.11	0.48	-6.22	37.14	34.80	27.84
1992	36.57	-0.65	-1.25	-0.36	0.90	1.60	1.58	1.79	1.52	-0.72	-1.36	-7.63	33.74	37.07	26.62
1993	42.83	-0.72	-1.14	-0.33	0.57	1.18	1.31	1.34	0.92	0.27	-0.65	-7.45	34.89	35.34	28.89
1994	25.00	0.02	-2.17	-0.23	0.11	0.03	-0.26	0.09	0.31	0.81	0.56	-6.04	38.37	28.94	28.12
1995	16.99	1.54	0.21	0.05	-0.23	1.55	2.17	1.64	0.98	-1.79	-0.14	-6.58	35.94	33.07	20.51
1996	21.03	-1.05	0.71	0.13	-0.53	-1.32	-0.41	-1.11	-0.82	-0.25	-0.33	-6.73	35.61	30.50	25.18
1997	25.82	0.41	-0.70	-0.02	1.16	0.49	0.77	0.61	1.16	0.58	-0.33	-6.73	34.82	30.73	25.18
1998	32.48	0.04	1.84	-0.22	-0.09	-0.04	2.23	0.59	-0.15	-2.24	-0.36	-6.84	36.27	35.20	25.74
1999	19.65	1.69	-0.17	0.12	-0.49	-2.49	-1.34	-1.80	-1.57	1.27	0.67	-7.26	38.72	21.04	28.94
2000	9.18	1.42	0.47	0.16	-0.28	-1.00	-1.66	-1.24	-0.74	3.69	0.53	-5.14	37.10	22.23	18.58
2001	7.42	2.44	0.79	0.10	-0.71	-1.04	-1.56	-0.89	-1.63	2.08	0.53	-5.14	37.96	23.62	22.74
2002	20.14	0.92	0.98	0.27	0.05	-0.15	0.35	0.34	-0.81	-0.12	0.47	-7.25	36.17	26.29	23.25
2003	34.78	1.50	0.60	-0.06	0.04	-1.22	-0.01	-1.01	-0.52	-0.96	1.11	-6.39	37.06	29.85	25.70
2004	28.40	0.75	0.21	-0.07	0.69	-0.25	-0.10	-0.06	-0.43	0.10	0.14	-7.18	35.30	26.99	21.75
2005	21.59	1.03	0.76	0.44	0.72	-0.16	0.68	0.27	-0.82	-0.47	0.14	-7.18	34.53	24.89	25.40
2006	15.01	0.49	0.30	0.06	-0.88	-0.87	-0.13	-0.62	-1.20	0.20	1.06	-7.22	38.97	25.99	20.19
2007	10.09	1.26	3.14	-0.10	0.18	-0.22	-0.16	-0.21	-1.21	1.12	0.24	-5.42	35.94	22.85	20.74

Table 3. Time series of regional monthly average rainfall (from April to June) and value of predictors

2.2.3 Neural information processing systems

Artificial neural networks (ANNs) form a class of systems that is inspired by biological neural networks. They usually consist of a number of simple processing elements, called neurons that are interconnected to each other. In most cases one or more layers of neurons are considered that are connected in a feed forward or recurrent way (Zurada 1992, Grossberg 1988, Lippmann 1987). In trying to understand the emergence of the new discipline of neural networks it is useful to look at some historical milestones in Table 4 (Johan et al. 1997).

2.2.4 Basic neural network architectures

The best known neural network architecture is the multilayer feedforward neural network (multilayer perceptron). It is a static network that consists of a number of layers: input

layer, output layer and one or more hidden layers connected in feedforward way (see e.g. Zurada 1992).

One signal neuron makes the simple operation of a weighted sum of the incoming signals and a bias term (or threshold), fed through an activation function σ and resulting in the output value of the neuron. A network with one hidden layer is described in matrix-vector notation as

$$y = W\sigma(V_x + \beta), \tag{13}$$

Or in elementwise notation:

$$y_i = \sum_{r=1}^{n_h} \omega_{ir}\sigma(\sum_{j=1}^{m} v_{rj}x_j + \beta_r) \quad i = 1,...,l. \tag{14}$$

Here $\chi \in$ Rm is the input and y $\in$ Rl the output of the network and the nonlinear operation σ is taken elementwise. The intererconnection matrices are $W \in \Re^{l \times n_h}$ for the output layer $V \in \Re^{n_h \times m}$ for the hidden layer, $\beta \in \Re^{n_h}$ is the bias vector (thresholds of hidden neurons) with n_h the number of hidden neurons.

Year	Network	Inventor /Discoverer
1942	McCulloch-Pitts neuron	McCulloch, pitts
1957	Perceptron	Rosenblatt
1960	Madaline	Widrow
1969	Cerebellatron	Albus
1974	Back propagation network	Werbos, parker, Rumelhart
1977	Brain state in a box	Anderson
1978	Neocognitron	Fukushima
1978	Adaptive Resonance Theory	Carpenter, Grossberg
1980	Self-organizing map	Kohonen
1982	Hopfield	Hopfield
1985	Bidirectional assoc. mem.	Kosko
1985	Boltzmann machine	Hinton, Sejnowsky
1986	Counterpropation	Hecht- Nielsen
1988	Cellular neural network	Chua, yang

Table 4. The best known artificial neural network architectures together with their year of introduction and their inventor/ discoverer. See Hecht Nielsen (1988) for part of this table (Johan et al, 1997).

Fig. 5 shows a multilayer perceptron, which is a static nonlinear network that consists of a dummy input layer, an output layer and two hidden layer. A layer consists of a number of McCulloch-pitts neurons that perform the operation of a weighted sum of incoming signals, feeded through a saturation-like nonlinearity. One hidden layer is sufficient in order to be universal approximators for any continues nonlinear function (Johan et al. 1997).

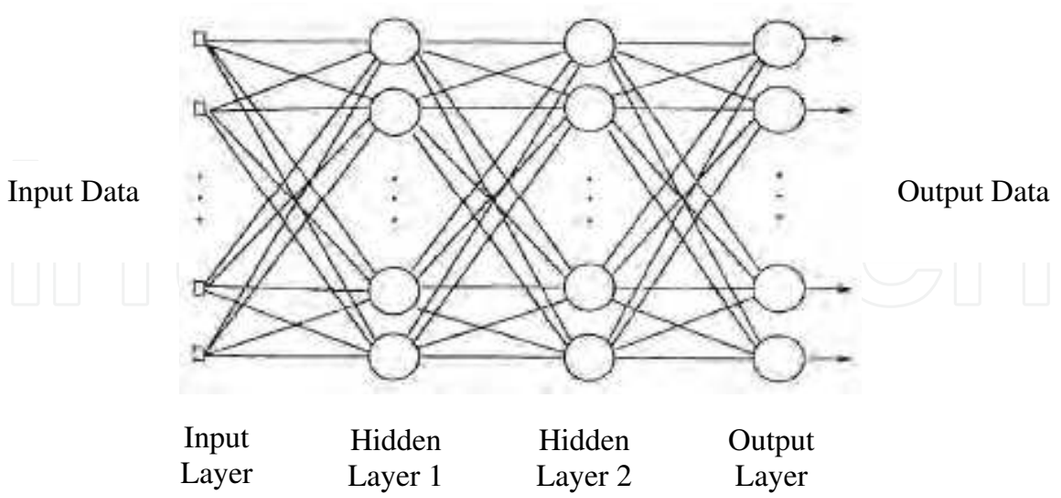

Fig. 5. Multilayer perceptron neural network (Johan et al, 1997).

For a network with two hidden layers (see Fig. 5):

$$y = W.\sigma(V_2.\sigma(V_1 x + \beta_1) + \beta_2) \tag{15}$$

Or:

$$y_i = \sum_{r=1}^{n_{h2}} w_{ir}\sigma(\sum_{s=1}^{n_{h1}} v_{rs}^{(2)}\,\sigma(\sum_{j=1}^{m} v_{sj}^{(1)} x_j + \beta_s^{(1)}) + \beta_r^{(2)}), \quad i = 1,...,l. \tag{16}$$

The interconnection matrices are $W \in \Re^{l \times n_{h2}}$ for the output layer, $V_2 \in \Re^{n_{h2} \times n_{h1}}$ for the second hidden layer and $V_1 \in \Re^{n_{h1} \times m}$ for the first hidden layer. The bias vectors are $\beta_2 \in \Re^{n_{h2}}$, $\beta_1 \in \Re^{n_{h1}}$ for the second a first hidden layer respectively. In order to describe a network with L layer (L-1 hidden layers, because the input layer is a 'dummy' layer), the following notation will be used in the sequel.

$$x_i^l = \sigma(\xi_i^l), \tag{17}$$

$$\xi_i^l = \sum_{j=1}^{N_l} w_{ij}^l x_j^{l-1} \tag{18}$$

Where $l = 1,...,L$ is the layer index, N_l denotes the number of neurons in layer l and x_i^l is the output of the neurons at layer l. The thresholds are considered here to be part of the interconnection matrix, by defining additional constant inputs.

The choice of the activation function σ may depend on the application area. Typical activation functions are shown in Fig. 6.

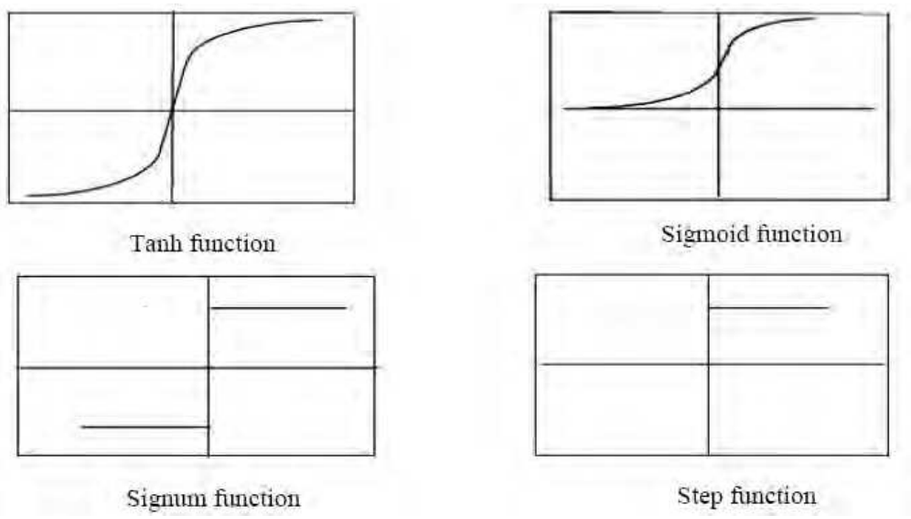

Fig. 6. Some possible activation functions for the neurons in the multilayer perceptron (Johan et al, 1997).

Fig. 6 shows some possible activation functions for the neurons in the multilayer precipitation. In this paper, we take the hyperbolic tangent function tanh. Note that this is a static nonlinearity that belongs to the sector [0, 1].

For applications in modeling and control the hyperbolic tangent functions:

$$\tanh(x) = (1 - \exp(-2x)) / (1 + \exp(-2x)) \tag{19}$$

Is normally used. In case of a 'tanh' the derivative of the activation function is:

$$\sigma' = 1 - \sigma^2 \tag{20}$$

The neurons of the input layer have a linear activation function.

A network that has received a lot of attention recently in the field of neural networks is the redial basic function network. This network can be described as:

$$y = \sum_{i=1}^{n_h} w_i g(\|x - c_i\|) \tag{21}$$

With $x \in \Re^m$ the input vector and $y \in \Re$ the output (models with multiple outputs are also possible). The network consists of one hidden layer with n_h hidden neurons. One of the basic differences with the multilayer perceptron is in the use of the activation function. In many cases one takes a Gaussian function for g, which is radially symmetric with respect to the input argument. The output layer has output weights $\omega \in \Re^{n_h}$. The parameters for the hidden layer are the centers $c_i \in \Re^m$ (Johan et al. 1997).

2.2.5 Recurrent neural network model

In recurrent neural network, some outputs of the nodes (output nodes or hidden nodes) are fed back to the previous layers. Most commonly used recurrent neural networks are external

recurrent neural networks (Fig.7). In this scheme, the outputs of a neural network are fed back to form a part of its input layer. Another recurrent scheme is internal recurrent neural networks, in which the outputs of hidden nodes (instead of output nodes) are fed back to the input layer (Fig.8) (Aoyama et al, 1999).

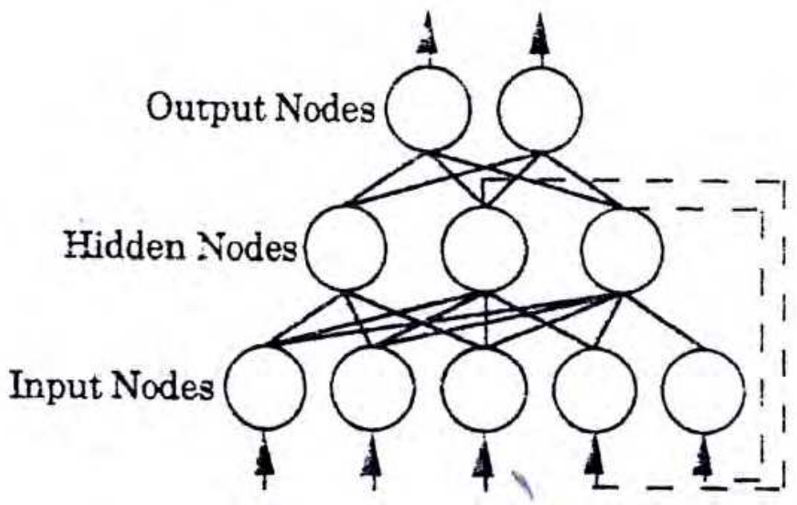

Fig. 7. External recurrent neural networks (Aoyama et al, 1999).

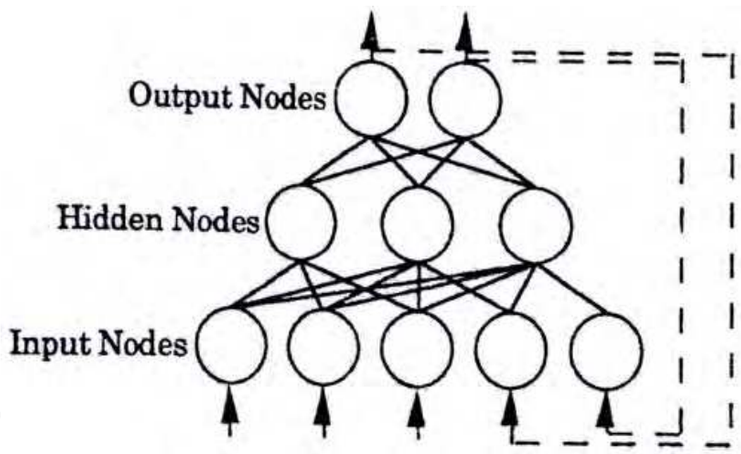

Fig. 8. Internal recurrent (state space) neural networks (Aoyama et al, 1999).

After various runs to test the network and the number of neurons of the hidden layer and different activation functions in the hidden and output layers, eventually found out that the final model with its one input layer, one hidden layer and one output layer (average regional rainfall) had the least error so in this research, used it as the main model. The numbers of the neurons in the input, hidden and output layers is fourteen, four and one respectively (14-4-1). The hidden layer activation function is a function of the hyperbolic tangent and the output layer activation function is a function of the linear hyperbolic tangent.

To assess the accuracy of the model, the index of Root Mean Square Error (RMSE) has been used which is calculated by the following formula:

$$RMSE = \sqrt{\frac{\sum_{i=1}^{n} (O_i - e_i)^2}{n}} \quad (22)$$

In the above formula, RMSE is Root Mean Square Error, O_i and e_i are the observed and predicted value of the variable respectively in the point i and n is number of network outputs.

3. Results and discussion

3.1 Predicting spring rainfall by means of artificial neural networks

In this study, Pearson Correlation Method has used to obtain meteorological predictors which affect regional rainfall. Thus, all the predictors which have shown a correlation with %5 level of significance in the period between October and March have been used as predictors in the structure of the rainfall forecast model. After numerous checking, it became clear that the optimum effect of predictors is when the period between October and March is used. Therefore, the following predictors in the period between October and March were used as predictors in rainfall forecast models: 1) SST Central Atlantic, 2) SST Western Mediterranean, 3) ΔSST Aral Lake, 4) ΔSST Labrador Sea, 5) SLP Northern Persian Gulf, 6) SLP Oman Sea, 7) SLP Southern Persian Gulf 8) SLP Southern Red Sea, 9) ΔSLP Between Eastern Mediterranean and Oman Sea, 10) air temperature at 700-hPa level in the region of index factor 2 in 5×5 degrees spatial resolution (Fig. 9), 11) air temperature at 700-hPa level in the index region of factor 3 in 5×5 degrees spatial resolution (Fig. 9), 12) precipitable water content in the index region of factor 10 in 10×10 degrees spatial resolution (Fig. 10), 13) relative humidity at 300-hPa level in the region of factor 2 in 5×5 degrees spatial resolution (Fig. 11), 14) relative humidity at 300-hPa level in the region of factor 4 in 5×5 degrees spatial resolution (Fig. 11). The variables which used as predictors in the rainfall forecast models show in the Table 5.

The above model divides the data into three different sections, namely, training data, validation data and testing data. The data belonging to 38 years were in turn divided into 19 years (1970– 1988) of training data, 9 years (1989–1997) of validation data and 10 years (1998–2007) of testing data. In the other words, from the whole set of historical data, two-thirds (1970-1997) were considered as calibration data, and one-third (1998 – 2007) as testing data. There is a clear analogy between the neural network weights and the parameters of other modeling approaches, and between the learning set and what we have before calles a period of calibration data. Work in neural networks often does not draw this analogy but it is a useful one in that just as an increase in the number of parameters gives a model more degrees of freedom in calibration but may result in over parameterization with respect to information in the data set, so in a neural network an increase in the number of layers, nodes and interconnections will also result in more degrees of freedom in fitting the learning set, also with the possibility of over parameterization (Beven 2001). Table 6 presents the results of the calibration period of the rainfall forecast model. As is shown, the minimum mean-square error after 1000 learning epochs is 0.169. Also, the maximum mean-square error is 0.169. In the other words, at this stage in the epoch of 1000, the network shows the maximum error. The minimum mean-square error of the validation epoch in the epoch of 3 is 0.234. The results of the prediction model are illustrated in Table 7 and Fig. 12. It is to be

noted that these results were presented for the years 1998 to 2007, which was the testing epoch of the model. The features of this model have been presented in Table 8.

Symbol	The Name of Predictor	Time	Correlation Coefficient with the average regional rainfall	P-value
(X1)	SST Central Atlantic	Oct-Mar	-0.31	0.05
(X2)	SST Western Mediterranean	Oct-Mar	-0.38	0.01
(X3)	ΔSST Aral Lake	Oct-Mar	-0.35	0.03
(X4)	ΔSST Labrador Sea	Oct-Mar	0.36	0.02
(X5)	SLP Northern Persian Gulf	Oct-Mar	0.31	0.05
(X6)	SLP Oman Sea	Oct-Mar	0.38	0.01
(X7)	SLP Southern Persian Gulf	Oct-Mar	0.31	0.05
(X8)	SLP Southern Red Sea	Oct-Mar	0.34	0.03
(X9)	ΔSLP Between Eastern Mediterranean and Oman Sea	Oct-Mar	-0.32	0.04
(X10)	air temperature at 700-hPa level in the region of index factor 2 in 5°×5° degrees spatial resolution (Fig. 9)	Oct-Mar	-0.38	0.01
(X11)	air temperature at 700-hPa level in the region of index factor 3 in 5°×5° degrees spatial resolution (Fig. 9)	Oct-Mar	-0.45	0.004
(X12)	precipitable water in the region of index factor 10 in 10°×10° degrees spatial resolution (Fig. 10)	Oct-Mar	-0.31	0.05
(X13)	relative humidity at 300-hPa level in the region of index factor 2 in 5°×5° degrees spatial resolution (Fig. 11)	Oct-Mar	0.45	0.004
(X14)	relative humidity at 300-hPa level in the region of index factor 4 in 5°×5° degrees spatial resolution (Fig. 11)	Oct-Mar	0.46	0.003

Table 5. Selected predictor variables which used in the rainfall prediction model

Best Networks	Training	Cross Validation
Epoch	1000	3
Minimum Mean Squared Error	0.169	0.235
Final Mean Squared Error	0.169	0.426

Table 6. Minimum & Maximum Error in Training and Validation Epochs

As Table 8 shows, the mean square error is 46.5 and the normalized mean square error is 0.55. Also, the mean absolute error for this model was calculated to be 6.15 millimeters. The minimum absolute error is 0.13 millimeter and the maximum absolute error is 10.9 millimeters. Also, the correlation coefficient between observed and predicted rainfall for the model is 0.79. The root mean square error for this model was calculated to be 6.8 millimeters.

Year	Observed rainfall	Predicted rainfall
1998	32	27
1999	19	15
2000	9	15
2001	7	15
2002	20	15
2003	34	24
2004	28	17
2005	21	15
2006	15	15
2007	10	15

Table 7. Rainfall prediction in the region under study by means of neural network model

Performance	Y (mm)
Mean Squared Error	46.54
Normalized Mean Squared Error(MSE/variance desired output)	0.55
Mean Absolute Error	6.15
Minimum Absolute Error	0.13
Maximum Absolute Error	10.98
Linear correlation coefficient	0.79

Table 8. The features of artificial neural network model

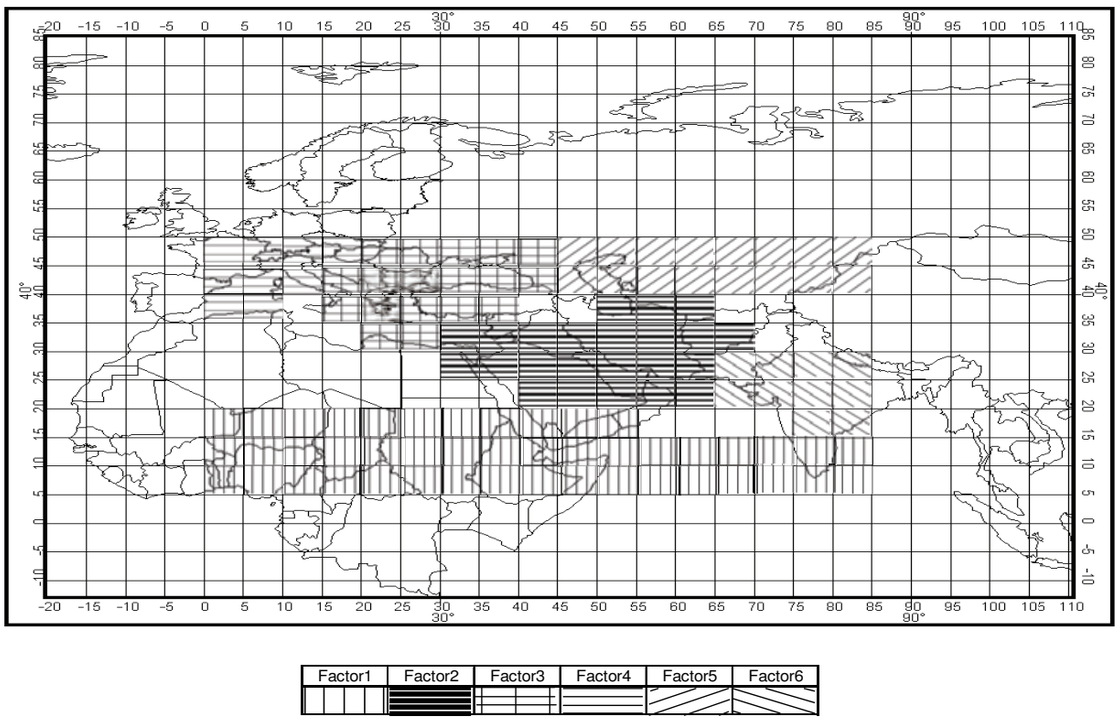

Fig. 9. The index areas detected by factor analysis at the temperature of 700-hPa level in the period October to March in networks of 5×5 degrees spatial resolution (Fallah Ghalhary et al, 2010)

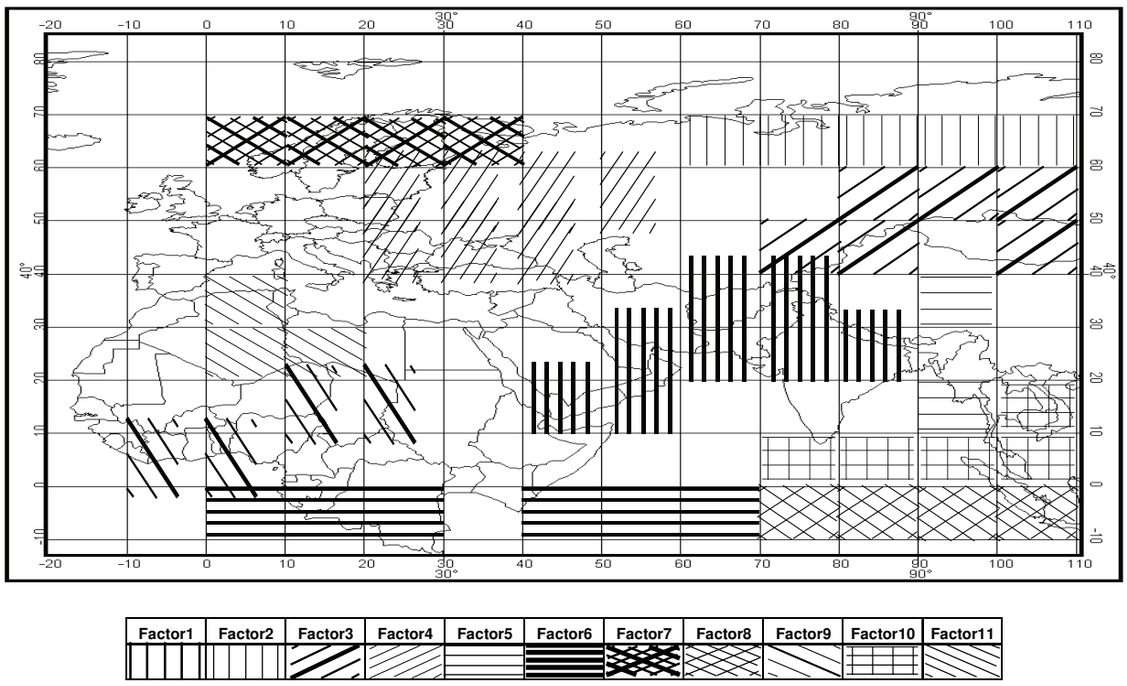

Fig. 10. The detected areas of precipitable water in the period October to March in networks of 10×10 degrees spatial resolution (Fallah Ghalhary et al, 2010)

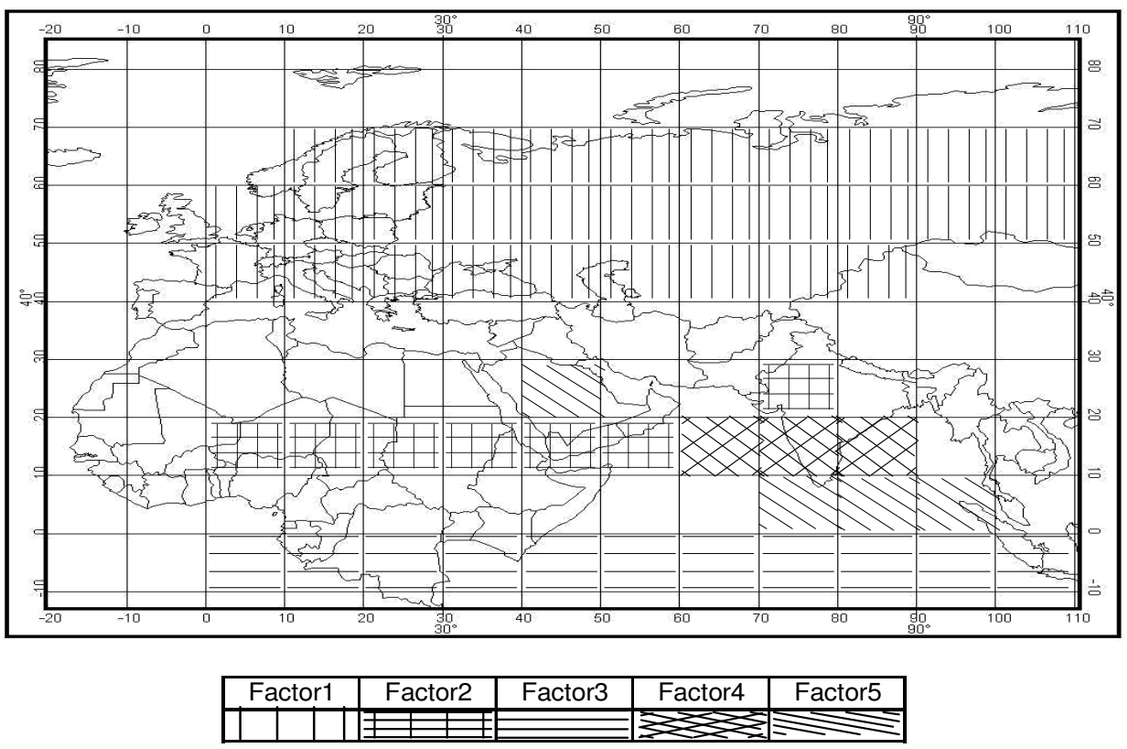

Fig. 11. The detected areas of relative humidity at 300-hPa level in networks of 5×5 degrees spatial resolution (Fallah Ghalhary et al, 2010)

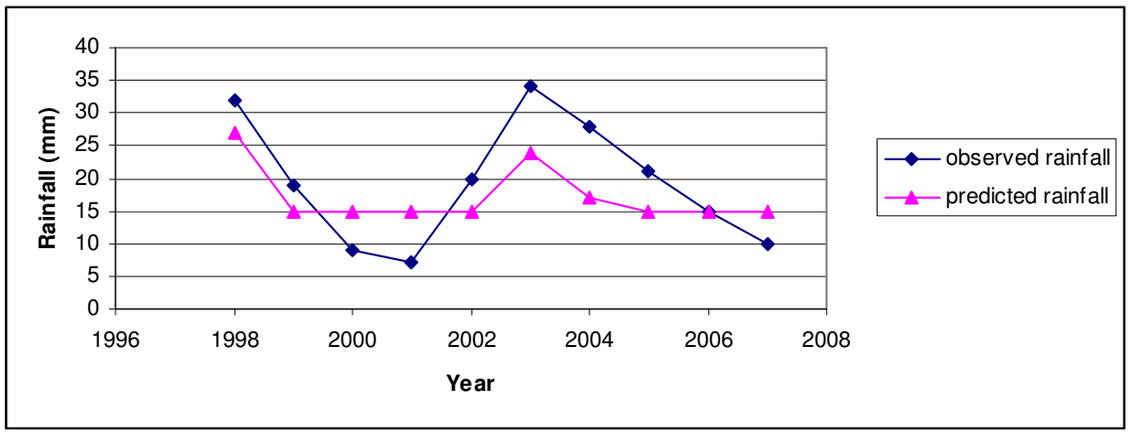

Fig. 12. Comparison of the observed and predicted rainfall in the region under study by means of artificial neural network model

The analysis of the results shows that the model is basically incapable of predicting rainfall in dry or wet extreme years. This is due to the fact that these extreme years have not been repeated in the calibration epoch of the prediction model and, for this reason, the model is not able to predict these extreme years. It must be noted that the minimum rainfall in the rainfall time series occurred in 2000 and 2001. To remove this problem, we must train the model with these extreme data. For this reason and in order to enable the neural network model to predict seasonal rainfall in such a way that it can be applied to all cases including dry, wet and normal years, we deleted the years 1998 and 2000 as the two extreme years in the test epoch of the model. One represents the dry extreme year and the other the wet extreme year. These two years were replaced by other data. They were taken out of the testing data and transferred into the training data and calibration epoch of the model. The results of the calibration epoch of the rainfall forecast model have been illustrated in Table 9. It is indicated that the minimum training error in the epoch of 17 is 0.108. The ultimate training error is 0.175. Also, the minimum validation error in the epoch of 1 is 0.087 and the ultimate validation error is 0.399. As the data show the accuracy of the model in detecting all dry, wet and normal years has amazingly increased. We can see that the accuracy of the model is higher than the previous model, as shown in Fig. 13, changes in the type of training data have affected the results of rainfall forecast model and that this model can estimate rainfall with higher accuracy.

Best Networks	Training	Cross Validation
Epoch	17	1
Minimum Mean Squared Error	0.108	0.087
Final Mean Squared Error	0.175	0.399

Table 9. Minimum and maximum error in training and validation epochs after modifying the network with proper historical data.

The observed and predicted rainfall by the model after modifying the input vector of the model in the training epoch has been presented in Table 10. the accuracy of the model has highly increased in this case and the root mean-square error has reached 2.5 millimeter, which indicates the high efficiency of the model in predicting rainfall in the area under study. The

features of this model have been presented in Table 11. The mean-square error is 6.7 millimeter and the normalized mean-square error is 0.12. Furthermore, the mean absolute error for this model was equal to 2.12 millimeters. The minimum absolute error was 0.03 millimeter and the maximum absolute error was 4.97 millimeters. The correlation coefficient between observed and predicted rainfall was 0.95, which is very reasonable. Fig. 14 shows the observed values of rainfall versus predicted values. The equation of the regression line for the changes in the values of observed versus predicted rainfall is as follows:

Observed Rainfall (mm) = 0.05 + 0.93 Predicted Rainfall

Year	Observed rainfall	Predicted rainfall
1996	21	22
1997	25	27
1998	32	35
1999	19	18
2001	7	7,7
2002	20	22
2004	28	25
2005	21	26
2006	15	15
2007	10	14

Table 10. Rainfall forecast in the region under study after modifying the network with historical data

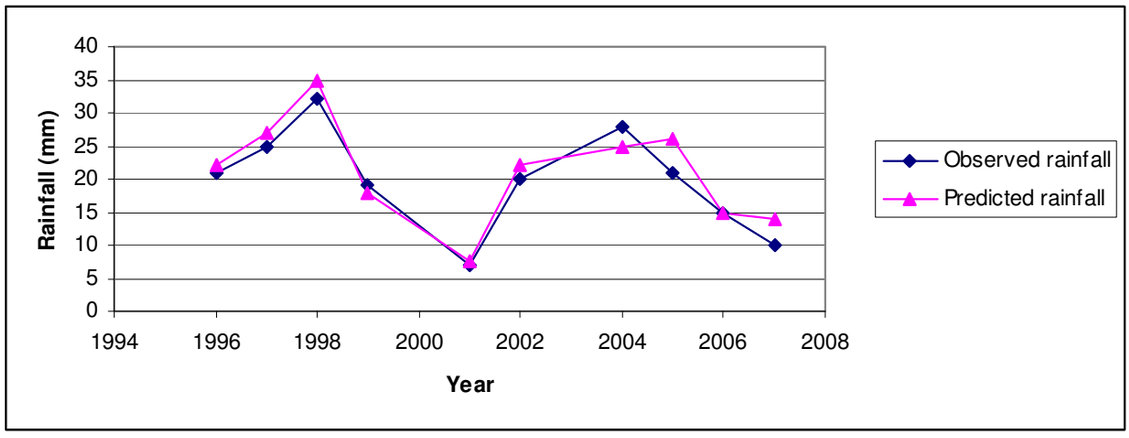

Fig. 13. Comparison of observed and predicted rainfall in the region under study by artificial neural network model after modifying the network with historical data.

the observations of the linear regression between observed values of rainfall and predicted values and the results of the variance analysis of the linear regression between the observed values of rainfall and predicted values have been summarized in Table 12 and Table 13 respectively. As we can see in Table 12, considering the confidence range of %99 of the linear regression between the observed values of rainfall and predicted values, the root mean-square error was calculated to be 2.46 millimeters. Table 13 shows that the F ratio is significant at %1 level, which is indicative of a strong relation between the changes in the

observed values of rainfall versus predicted values. The significance test of the gradient of the regression line between the true values of rainfall and the values predicted by the model has also been done (Table 14). As observed here, the gradient of the regression line is also significant at %1 level. The P-value for the significance test of the gradient of the regression equation was smaller than 0.0001.

Performance	Y (mm)
Mean Squared Error	6.73
Normalized Mean Squared Error(MSE/variance desired output)	0.12
Mean Absolute Error	2.12
Minimum Absolute Error	0.03
Maximum Absolute Error	4.97
Linear correlation coefficient	0.95

Table 11. Features of artificial neural network after modifying the network with historical data

Variable	Value
RSquare	0.908079
RSquare Adj	0.896589
Root Mean Square Error	2.466808
Mean of Response	19.8
Observations (or Sum Wgts)	10

Table 12. Summary of the observations of the linear regression between the true values of rainfall and predicted values

Source	DF	Sum of Squares	Mean Square	F Ratio
Model	1	480.91887	480.919	79.0317
Error	8	48.68113	6.085	Prob > F
C. Total	9	529.60000		<.0001

Table 13. The variance analysis of the linear regression between the true values of rainfall and predicted values

Term	Estimate	Std Error	t Ratio	Prob>|t|
Intercept	-0.075552	2.367907	-0.03	0.9753
Predicted rainfall (mm)	0.9388546	0.105608	8.89	<.0001

Table 14. Summary of the statistical observations of the estimation of the parameters of the model

Model	RMSE	Maximum Absolute Error	Minimum Absolute Error
ANN Model	6.82	10.98	0.13
Modified ANN Model	2.5	4.97	0.03

Table 15. Statistical comparative of two models

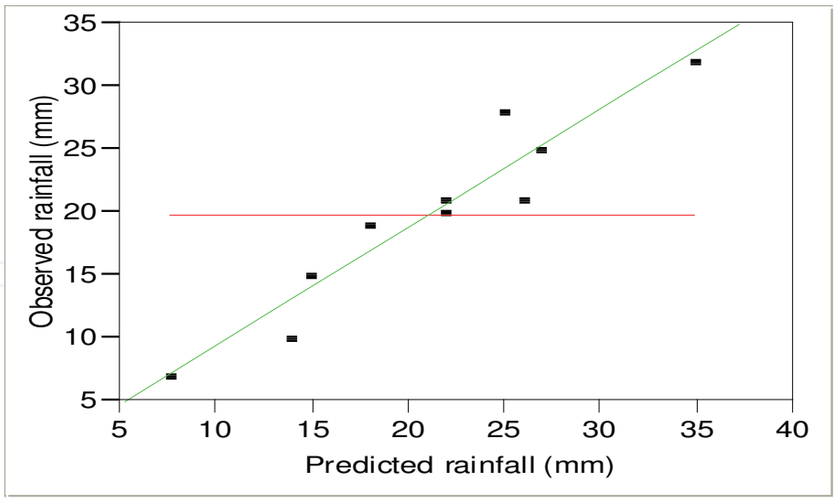

Fig. 14. Changes in the true values of rainfall versus predicted values. The slanted line is the regression line

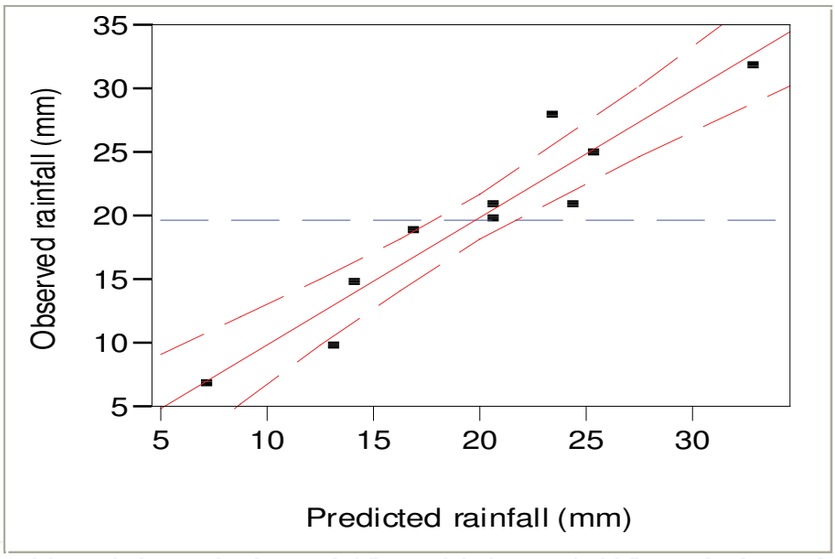

Fig. 15. The confidence range of %99 for changes of the observed rainfall versus predicted values

The confidence range of %99 for the changes of the observed rainfall versus the predicted values has been illustrated (Fig. 15). Here again, the changes of the observed rainfall and the predicted rainfall shows a close correspondence, being significant at 0.01 level. Fig. 16 Displays the changes in the values of residuals versus predicted values of rainfall. Here again, the changes in the values of residuals versus predicted values of rainfall are completely accidental and normal, indicating the high accuracy of the model in predicting rainfall. In sum, the analysis of the results indicates that the difference between the observed and predicted rainfall is within a reasonable range; moreover, the model has been able to predict rainfall in all years with an acceptable error. The root mean-square error for this model was 2.5 millimeter, which is very small, indicating the accuracy of the model in predicting rainfall. We can conclude from

the above discussion that the variables used in the model have been able to detect the distribution pattern of rainfall in the region with great ease and accuracy. We can also decide that the model can be successfully used for predicting rainfall in spring.

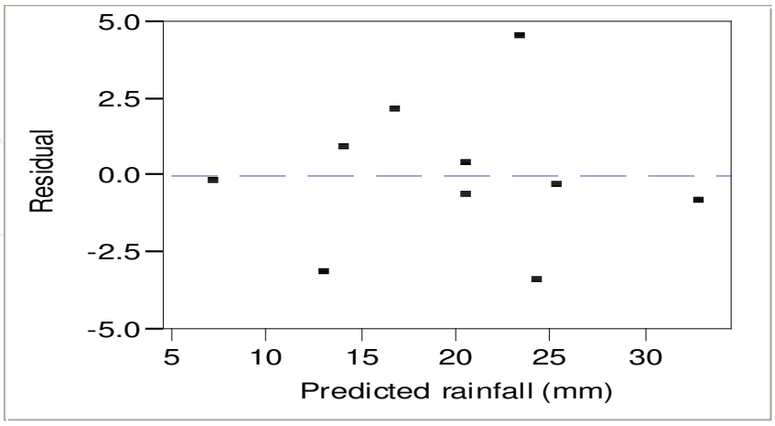

Fig. 16. Changes of the values of residuals versus predicted values of rainfall in terms of millimeter

4. Conclusion

Based on the obtained results, we can conclude that ANN models were successful in the prediction of spring rainfall, but the ANN model has higher accuracy after the revision of training data with a root mean square error of 2.5 milliliters. This is clearly observable in Fig.13, ANN model after the revision of training data has been more successful than the before. Table 15 shows the results of two ANN models to predicting the amount of the rainfall in the area under study. At the end, we can result that the variables entering rainfall prediction models have been well able to detect the rainfall distribution patterns in the region and can be used in rainfall prediction patterns in the region. This plays a vital role in the management and planning of drink and agriculture water resources. Considering these predictions, we can plan future policies for optimizing the costs and possibilities for maximum efficiency.

5. Acknowledgement

This paper presents part of the findings of the research project "Predicting spring rainfall in Khorasan Razavi Province based on meteorological predictors by means of fuzzy logic, artificial neural networks and adaptive neuron-fuzzy networks" by the same author. The author greatly appreciates the cooperation of the directors and managers of the "Climatological Research Institute" who provided the possibilities required for the completion of this project.

6. References

Abraham A., Sajith N., Joseph B. (2001). Will We Have a Wet Summer? Long-term Rain Forecasting Using Soft Computing Models: Modelling and Simulation, Publication of the Society for Computer Simulation International, Prague, Czech Republic, 1044-1048

Alijani B., 2006. Synoptic Climatology: 2nd ed. Samt Publication, Tehran, Iran, 258 pp.

Aoyama A., Doyle F. J., Vankat V. (1999). Fuzzy neural network systems techniques and their applications to nonlinear chemical process control systems, Academic press, 2:485-493.

Beven K., 2001. Rainfall-Runoff Modelling, John Wiley & Sons, LTD, First Ed, ISBN: 978-0-470-86671-9, PP.360.

Cavazos T., 2000. Using Self-Organizing Maps to Investigate Extreme Climate Event: An Application to wintertime Rainfall in the Balkans, J. Climatol. 13: 1718-1732.

Choi L., 1999. An application hydroinformatic tools for rainfall forecasting: Thesis (PhD). University of New South Wales (Australia), 752 pp.

Cressie, N., 1990. The origins of Kriging. Mathematical geology. 22. 239-252.

Cressie, Noel A.C., 1993. Statistics for Spatial Data, Revised Edition. New York: John Wiley & Sons, Inc. 900 p.

Davis J.C., 1990. Statistics and Data Analysis in Geology, John Wiley & Sons Inc, ISBN-10: 0471198951, PP. 564.

Ducan A.J., 1974. Quality Control and Industrial Statistics. Richard D. IRWIN, INC., 4 editions.

Fallah Ghalhary G. A., Habibi Nokhandan M., Mousavi Baygi M., Khoshhal J. and Shaemi Barzoki A. (2010). Spring rainfall prediction based on remote linkage controlling using adaptive neuro-fuzzy inference system (ANFIS), Theor Appl Climatol, 101:217–233.

Feller W., 1968. An Introduction to Probability Theory and its Applications, 1. John Wiley & Sons, Inc., 3 rd edition.

Ford J.K., MacCallum R.C. and Tait M. (1986). The Application of Exploratory Factor-Analysis in Applied- Psychology - a Critical-Review and Analysis. Personnel Psychology, 39(2):.291-314.

Gandin L.S., 1963. Objective analysis of meteorological fields. Gidrometeorologicheskoe Izdatel'stvo (GIMIZ), Leningrad (translated by Israel program for scientific translations, Jerusalem, 1965)

Gorsuch R.L., 1997. Common Factor-Analysis versus Component Analysis - Some Well and Little Known Facts, Multivar Behav Res, 25(1): 33-39.

Grossberg S., 1988. Nonlinear neural networks: principles, mechanisms and architectures. Neural Networks, 1: 17-61.

Guibas L.J. and Odlyzko A.M. (1980). Long Repetive Patterns in Random Sequences. Z. Wahrscheinlichkeitstheorie, 53: 241-262.

Halid H. and Ridd P. (2002). Modelling Inter-Annual Variation of Local Rainfall Data: Using a Fuzzy Logic Technique. Proceedings of International Forum on Climate Prediction, James Cook University, Australia. First Proof. Pages, 166-170.

Haltiner G.J. and Williams R.T. (1980). Numerical Prediction and Dynamic Meteorology. 2nd Edition. New York, Wiley & Sons, PP. 447.

Hecht Nielsen R., 1988. Neurocomputer applications in NATO ASI Series, NEURAL COMPUT, 41, Eds. R. Eckmiller, Ch.v.d.Malsburg, Springer-Verlag.

Iseri Y., Dandy G.C., Maier H.R., Kawamura A. and Jinno K. (2005). Medium Term Forecasting of Rainfall using Artificial Neural Networks, Neural Networks, 1834-1840.

Johan A.K.S., Joos P.L.V. and Bart L.R.D.M. (1997). Artificial Neural Networks for Modelling and Control of Non-Linear Systems, Kluwer Academic Publishers, second Ed, PP.235. ISBN: 0-7923-9678-2.

Journel A.G. and Huijbregts C.H.J. (1978). Mining geostatistics, Academic press, London.
Kawamura A., McKerchar A.I., Spigel R. H. and Jinno K. (1998). Chaotic characteristics of the Southern Oscillation Index time series, Journal of Hydrology. 204: 168-181.
Knuth D.E., 1981. The Art of Computer Programming, 2: Semi numerical Algorithms. Addison-Wesley, Reading, MA, 2nd edition.
Kolmogorov A.N., 1941. Interpolation and extrapolation of stationary random sequences. Izvestiia Akademii Nauk SSSR, Seriia Matematicheskiia, 5, 3-14. [Translated, 1962, Memo Rm-3090-PR, Rand Corp, Santa Monica, CA.,].
Kridge D.G., 1951. A statistical approaches to some basic mine valuation problems on the Witwatersrand. Journal of the chemical, Metallurgical and Mining society of South Africa, 52, 119-139.
Laslett G.M. and McBratney A.B. (1990). Further comparison of spatial methods for predicting soil pH, Soil Sci. Soc. Am. J. 54, 1553-1558.
Lewis F.L., 1986. Optimal estimation. Wiley, New York.
Lippmann R.P., 1987. Introduction to computing with neural nets, IEEE ASSP magazine, April: 4-22.
Mantua N.J. Hare S.R., Zhang Y., Wallace J.M. and Francis R.C. (1997). A Pacific interdecadal climate oscillation with impacts on salmon production, Bulletin of the American Meteorological Society 78: 1069-1079.
Maria C., Haroldo F. and Ferreira N. (2005). Artificial neural network technique for rainfall forecasting applied to the Sao Paulo region. J. Hydrol , 301:146-162.
Matheron G., 1963. Principle of geostatistics, Economic Geology, 58, 1246-1266.
Matheron G., 1971. The theory of regionalized variables and its application. Cahiers du Centre de Morphologie Mathematique, No.5. Fontainebleau, France.
Nazemosadat M.J. and Cordery I. (2000). On the Relationship between ENSO and Autumn Rainfall in Iran. J. Climatol. 1: 47-62.
Philip G.M. and Watson D.F. (1986). Matheronian geostatistics-Quo vadis? Mathematical geology, 18, 93-117.
Pongracz R. and Bartholy J. (2006). Regional Effects of ENSO in Central/Eastern Europe, j. ADGEO. 6:133-137.
Silverman D. and Dracup J.A. (2000). Artificial neural networks and long-range precipitation prediction in California, J Appl Meteorol, 39: 57-66.
Trenberth K.E. and Hurrel J.W. (1994). Decadal atmosphere-ocean variations in the Pacific. Climate Dynamics 9: 303-319.
Weber D. and Englund E. (1992). Evaluation and comparison of spatial interpolators. Mathematical Geology 24:4, 381-391.
Wold H., 1938. A study in the analysis of stationary time series. Almqvist and Wiksells, Uppsala.
Wolfowitz J., 1944. Asymptotic distribution of runs up and down. Annals Math. Stat., 15: 163-165
Zhang Y., Wallace J.M. and Battisi D.S. (1997). ENSO-like interdecadal variability 1900-1993, Journal of Climate 10: 1004-1020.
Zurada J.M., 1992. Introduction to Artificial Neural Systems, West publishing company.
Zwiers F.W. and von Storch H. (2004). On the role of statistics in climate research. Int. J Climatol. 24: 665–680.

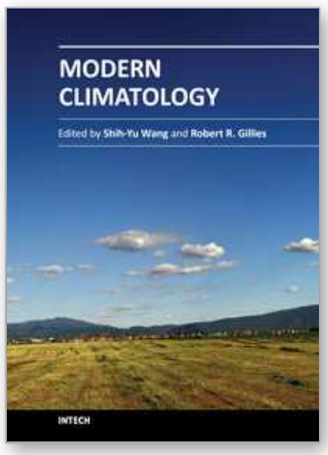

Modern Climatology

Edited by Dr Shih-Yu Wang

ISBN 978-953-51-0095-9
Hard cover, 398 pages
Publisher InTech
Published online 09, March, 2012
Published in print edition March, 2012

Climatology, the study of climate, is no longer regarded as a single discipline that treats climate as something that fluctuates only within the unchanging boundaries described by historical statistics. The field has recognized that climate is something that changes continually under the influence of physical and biological forces and so, cannot be understood in isolation but rather, is one that includes diverse scientific disciplines that play their role in understanding a highly complex coupled "whole system" that is the earth's climate. The modern era of climatology is echoed in this book. On the one hand it offers a broad synoptic perspective but also considers the regional standpoint, as it is this that affects what people need from climatology. Aspects on the topic of climate change - what is often considered a contradiction in terms - is also addressed. It is all too evident these days that what recent work in climatology has revealed carries profound implications for economic and social policy; it is with these in mind that the final chapters consider acumens as to the application of what has been learned to date.

INTECH
open science | open minds

InTech Europe
University Campus STeP Ri
Slavka Krautzeka 83/A
51000 Rijeka, Croatia
Phone: +385 (51) 770 447
Fax: +385 (51) 686 166
www.intechopen.com

InTech China
Unit 405, Office Block, Hotel Equatorial Shanghai
No.65, Yan An Road (West), Shanghai, 200040, China
中国上海市延安西路65号上海国际贵都大饭店办公楼405单元
Phone: +86-21-62489820
Fax: +86-21-62489821

IntechOpen